

# Vibration characteristics of two-stage planetary transmission system with thin-walled ring gear on elastic supports

JianYing Li <sup>1</sup>, QingChun Hu <sup>2\*</sup>, ChangFu Zong <sup>1</sup>, TianJun Zhu <sup>1</sup> and ZeXing Zhang <sup>1</sup>

<sup>1</sup> School of Mechanical and Automotive Engineering, Zhaoqing University, Zhaoqing 526061, China

<sup>2</sup> School of Mechanical and Automotive Engineering, South China University of Technology, Guangzhou 510640, China

School of Natural Science Fund Project (201728); Practical Teaching Reform Project (sjjx201627); Guangdong Province Natural Science Fund (2014A030311045)

Email: huqingchunscut@163.com

**Abstract.** A dual-clutch and dual-speed planetary gears mechanism of a hybrid car coupled-system is taken as research subject, in which the ring gear of planet set II is a thin-walled structure and the clutch friction plates of planet set II are used as its elastic supports. Based on the lumped parameter-rigid elastic coupled dynamic model of two-stage planetary transmission system with thin-walled ring gear on elastic supports, the motion differential equations are established and the dynamic responses are solved by the Runge-Kutta method considering each stage internal and external time-varying mesh stiffness. The vibration displacements of each stage ring gear have been affected differently in time-domain, the translational vibration displacement of the ring gear of planet set I are obviously more than the torsional vibration displacement, but it is opposite for the ring gear of planet set II; The translational and torsional vibration responses of each stage ring gear arrive the peak in low-frequency. The analysis results of this paper can enrich the theoretical research of multistage planetary transmission and provide guidance for dynamic design.

## 1. Introduction

Planetary gears mechanism is a key part of the transmission system of a hybrid car, which is often solved multi-power sources coupled problem [1,2]. Although many studies on the planetary gears are carried out, its vibration and noise is still an important research subject, such as dynamic modeling, natural frequency analysis and dynamic response solving, parameters stability in Refs. [3-11], in which the basic components and planet gears are seen as rigid bodies, and the support stiffness and time-variant meshing stiffness are considered. When the ring gear is a thin-walled structure, its elasticity should be taken into account in certain situations [12-15].

The dynamic characteristics of transmission system have been affected by the elastic deformations of thin-walled ring gear, so the ring gear is no longer seen as a rigid body by some researchers, the modal properties of planetary gears having elastic continuum ring gear are studied by the perturbation and a candidate mode method, in which the planet are spaced equally and unequally, and its parametric instability are analyzed in Refs. [16-18]. Zhang Jun et al [19,20] pointed out the elasticity of the ring gear has a certain influence on the dynamic characteristics of planetary gears. Tao Qing et



al[21] proposed a novel modeling method of rigid-flexible coupled planetary gear transmission systems that consist of rigid gear subsystems and elastic ring gear subsystems, its model is established by using the finite element method. Bao Heyun et al[22] established a translational-rotational dynamics model with meshing beyond pitch point in consideration of planetary gear sliding friction, time-varying mesh stiffness and damp, integrated mesh errors and flexible ring. Li Jianying and Hu Qingchun et al in Refs. [23,24] established the same lumped parameter-rigid elastic coupled dynamic model of two-stage planetary transmission system for a hybrid car through inter-stage coupled method, after including the elasticity of the ring gear of planet set II and simplifying its elastic supports. In Ref. [23], the natural frequencies are solved and the associated vibration modes are discussed, the rules are revealed which are the influences of the elastic supports stiffness and rim thickness of the ring gear of planet set II on natural frequencies of two-stage planetary transmission system, and the vibration modes are classified into seven types: I / II stage coupled rotational mode, I stage translational mode, I stage planet mode, II stage translational mode, II stage degenerate planet mode, II stage distinct planet mode and purely ring gear mode, its properties are summarized. In Ref. [24], the dynamic characteristics of two-stage planetary transmission system with thin-walled ring gear on elastic supports under different working conditions are discussed by the theoretical analysis and experimental testing.

In order to know the vibration characteristics of two-stage planetary transmission system with thin-walled ring gear on elastic supports, a dual-clutch and dual-speed planetary gears mechanism of a hybrid car coupled-system is taken as research subject in this paper, and its composition is described in detail in Refs. [23, 24], in which the ring gear of planet set II is a thin-walled structure and the clutch friction plates of planet set II are used as its elastic supports. The translational and torsional directions time-domain and frequency-domain vibration displacement of planet set I and II of two-stage planetary transmission system with thin-walled ring gear on elastic supports are solved by numerical method considering each stage internal and external time-varying mesh stiffness. The results of this paper can enrich the theoretical research of multistage planetary transmission and provide guidance for dynamic design.

## 2. The motion differential equations of planetary transmission with thin-walled ring gear on elastic supports [23, 24]

Two-stage planetary gears mechanism for a hybrid car is composed of planet set I and II, clutches  $c_1$ ,  $c_2$  and shell, there are three assumptions when modeling in this paper (Seen Refs.[23,24]). The carrier of planet set I is the input, the sun of planet set I and II is the output. The sun of planet set I and II connect together, the ring gear of planet set I and the carrier of planet set II connect together. Clutch  $c_1$  simultaneously control the ring gear of planet set I and the carrier of planet set II. Clutch  $c_2$  only control the ring gear of planet set II. Figure 1 is dynamic model of two-stage planetary system with thin-walled ring gear on elastic supports, its establishing method in detail can be seen Refs.[23,24].

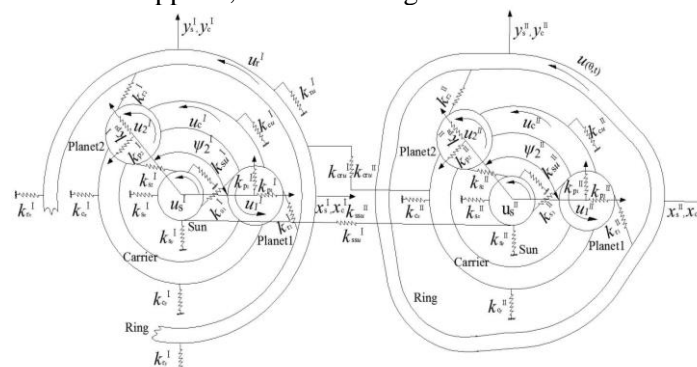


**Figure 1.** Dynamic model of two-stage planetary transmission system with thin-walled ring gear on elastic supports [23,24].

Establishing the motion differential equations of planet set I and II according to Newton's second law

$$M_e \ddot{u} + k_{\text{bend}} L_1 u + k_m^{\text{II}} L_2 u + k_m^{\text{II}} \sum_{n=1}^{N_{\text{II}}} L_3^n (x_n \sin \alpha_r - y_n \cos \alpha_r - u_n) = 0 \quad (1)$$

$$\begin{cases} m_r^i \ddot{x}_r^i - \sum_{n=1}^{N_i} k_{rn}^i \delta_{rn}^i \sin \psi_{rn}^i + \Delta_{rx}^i + \nabla_{rx}^i = 0 \\ m_r^i \ddot{y}_r^i + \sum_{n=1}^{N_i} k_{rn}^i \delta_{rn}^i \cos \psi_{rn}^i + \Delta_{ry}^i + \nabla_{ry}^i = 0 \\ \left[ I_r^i / (r_r^i)^2 \right] \ddot{u}_r^i + \sum_{n=1}^{N_i} k_{rn}^i \delta_{rn}^i + \Delta_{ru}^i + \nabla_{ru}^i = 0 \end{cases} \quad (2)$$

$$\begin{cases} m_c^i \ddot{x}_c^i + \sum_{n=1}^{N_i} k_{pn}^i (\delta_{nt}^i \sin \psi_n^i - \delta_{nr}^i \cos \psi_n^i) + k_{cx}^i x_c^i = 0 \\ m_c^i \ddot{y}_c^i - \sum_{n=1}^{N_i} k_{pn}^i (\delta_{nt}^i \cos \psi_n^i + \delta_{nr}^i \sin \psi_n^i) + k_{cy}^i y_c^i = 0 \\ \left[ I_c^i / (r_c^i)^2 \right] \ddot{u}_c^i - \sum_{n=1}^{N_i} k_{pn}^i \delta_{nt}^i + \Delta_{cu}^i = \frac{T_c^i}{r_c^i} \end{cases} \quad (3)$$

$$\begin{cases} m_s^i \ddot{x}_s^i - \sum_{n=1}^{N_i} k_{sn}^i \delta_{sn}^i \sin \psi_{sn}^i + k_{sx}^i x_s^i = 0 \\ m_s^i \ddot{y}_s^i + \sum_{n=1}^{N_i} k_{sn}^i \delta_{sn}^i \cos \psi_{sn}^i + k_{sy}^i y_s^i = 0 \\ \left[ I_s^i / (r_s^i)^2 \right] \ddot{u}_s^i + \sum_{n=1}^{N_i} k_{sn}^i \delta_{sn}^i + \Delta_{su}^i = -\frac{T_s^i}{r_s^i} \end{cases} \quad (4)$$

$$\begin{cases} m_n^i \ddot{x}_n^i + k_{rn}^i \delta_{rn}^i \sin \alpha_r^i - k_{sn}^i \delta_{sn}^i \sin \alpha_s^i + k_{pn}^i \delta_{rn}^i + \nabla_{nx}^i = 0 \\ m_n^i \ddot{y}_n^i - k_{rn}^i \delta_{rn}^i \cos \alpha_r^i - k_{sn}^i \delta_{sn}^i \cos \alpha_s^i + k_{pn}^i \delta_{rn}^i + \nabla_{ny}^i = 0 \\ \left[ I_n^i / (r_n^i)^2 \right] \ddot{u}_n^i - k_{rn}^i \delta_{rn}^i + k_{sn}^i \delta_{sn}^i + \nabla_{nu}^i = 0 \end{cases} \quad (5)$$

where  $M_e$  represents equivalent mass of the ring gear of planet set II;  $k_{\text{bend}}$  is bending stiffness of the ring gear of planet set II,  $k_{\text{bend}} = EI / R^3 (1 - \nu^2)$ , where  $E$  is Yong's modulus of the ring gear of planet set II,  $E = 2.07 \times 10^{11}$ ,  $\nu$  is Poisson's ratio of the ring gear of planet set II,  $\nu = 0.3$ ,  $R$  is neutral radius of the ring gear of planet set II,  $I$  is area moment of inertia of the ring gear of planet set II;  $L_1$ ,  $L_2$  and  $L_3$  are dimensionless operators (see Appendix of Refs.[23,24]).  $m_h^i$ ,  $I_h^i$  are mass and moment of inertia of component  $h$  of planet set  $i$ ;  $T_h^i$  is external torque of component  $h$  of planet set  $i$ ;  $\nabla_{ij}^i$ ,  $\nabla_{nj}^i$  represent elastic coupled term of the ring gear, the  $n^{\text{th}}$  planet in the  $j$  direction, respectively;  $\Delta_{ij}^i$  represent bearing coupled term of the ring gear in the  $j$  direction;  $\Delta_{hu}^i$  represent torsional coupled term of component  $h$  of planet set  $i$ . All coupled terms are

$$\begin{aligned} \nabla_{rx}^{\text{I}} = \nabla_{ry}^{\text{I}} = \nabla_{ru}^{\text{I}} = 0, \nabla_{rx}^{\text{II}} = \nabla_{ry}^{\text{II}} = \nabla_{ru}^{\text{II}} &= \left( \sum_{n=1}^{N_{\text{II}}} b_r \chi \right) \Big|_{\theta=\psi_n^{\text{II}}} \\ \nabla_{nx}^{\text{I}} = \nabla_{ny}^{\text{I}} = \nabla_{nu}^{\text{I}} = 0, \nabla_{nx}^{\text{II}} = \nabla_{ny}^{\text{II}} = \nabla_{nu}^{\text{II}} &= b_p \chi \Big|_{\theta=\psi_n^{\text{II}}} \end{aligned}$$

$$\Delta_{rx}^i = \begin{cases} k_{rx}^I x_r^I, i = I \\ \pi(k_{rbs} + k_{rus}) x_r^{II}, i = II \end{cases}, \Delta_{ry}^i = \begin{cases} k_{ry}^I y_r^I, i = I \\ \pi k_{rbs} y_r^{II}, i = II \end{cases}, \Delta_{ru}^i = \begin{cases} k_{ru}^I u_r^I + k_{cu}^I \frac{r_e}{r_r^I} \left( \frac{r_e}{r_r^I} u_r^I - \frac{r_e}{r_c^{II}} u_c^{II} \right), i = I \\ \frac{2\pi k_{rus}}{\cos^2 \alpha_r^{II}} u_r^{II}, i = II \end{cases}$$

$$\Delta_{su}^i = \begin{cases} k_{su}^I u_s^I + k_{ssu}^I \frac{r_b}{r_s^I} \left( \frac{r_b}{r_s^I} u_s^I - \frac{r_b}{r_s^{II}} u_s^{II} \right), i = I \\ k_{su}^{II} u_s^{II} + k_{ssu}^{II} \frac{r_b}{r_s^{II}} \left( \frac{r_b}{r_s^{II}} u_s^{II} - \frac{r_b}{r_s^I} u_s^I \right), i = II \end{cases}, \Delta_{cu}^i = \begin{cases} k_{cu}^I u_c^I, i = I \\ k_{cu}^{II} u_c^{II} + k_{cu}^{II} \frac{r_e}{r_c^{II}} \left( \frac{r_e}{r_c^{II}} u_c^{II} - \frac{r_e}{r_r^I} u_r^I \right), i = II \end{cases}$$

where  $\chi = \frac{\partial}{\partial \theta} \sin \alpha_r^{II} + \cos \alpha_r^{II}$ ,  $b_r = (-\sin \psi_m^{II}, \cos \psi_m^{II}, 1)^T$ ,  $b_p = (\sin \alpha_r^{II}, -\cos \alpha_r^{II}, 1)^T$ .  $r_c$  is connecting shaft radius of the ring

gear of planet set I with the planet of planet II,  $r_b$  is connecting shaft of the sun gear of planet set I with the sun gear of planet set II, all other symbol of equations (1) -(5) can be referred in Refs. [23,24].

The internal and external time-varying mesh stiffness with the  $n^{\text{th}}$  planet of planet set  $i$   $k_{sn}^i(t)$ ,  $k_m^i(t)$

$$k_{sn}^i(t) = \bar{k}_{sn}^i + 2\mu^i \sum_{l=1}^{\infty} (a_{sn}^{i(l)} \sin l\omega_m^i t + b_{sn}^{i(l)} \cos l\omega_m^i t), k_m^i(t) = \bar{k}_m^i + 2\varepsilon^i \sum_{l=1}^{\infty} (a_m^{i(l)} \sin l\omega_m^i t + b_m^{i(l)} \cos l\omega_m^i t) \quad (6)$$

where  $\bar{k}_{sn}^i$ ,  $\bar{k}_m^i$  are internal and external average mesh stiffness;  $2\mu^i$ ,  $2\varepsilon^i$  are peak to peak amplitudes of internal and external mesh stiffness variations;  $a_{h'n}^{i(l)}$ ,  $b_{h'n}^{i(l)}$  ( $h' = s, r$ ) are Fourier series expansion coefficient;  $l$  is Fourier series expansion number;  $\omega_m^i$  is mesh frequency [24].

### 3. Dynamic responses of planetary transmission with thin-walled ring gear on elastic supports

The Runge-Kutta method is used for numerical solutions of equations (1) -(6) in this paper and numbers of each stage planet are 4. The input shaft rotation speed  $n_c^I = 100r/\text{min}$  and the input load torque  $T_c^I = 35.2\text{Nm}$ , the ring gear of planet set I and the carrier of planet set II are fixed components, the numerical simulation parameters are shown in Table1.

**Table 1.** Parameters of two-stage planetary transmission system with thin-walled ring gear on elastic supports [23,24].

|               | Parameters                              | Ring gear | Carrier  | Sun gear | Planet |
|---------------|---|-----------|--|----------|--------|
| Planet set I  | Teeth                                   | 83        | —  | 33       | 25     |
|               | Pitch diameter/mm                       | 103.75    | —  | 41.25    | 31.25  |
|               | Base diameter/mm                        | 97.49     | 72.5   | 38.76    | 29.37  |
|               | Modulus/mm                              | 1.25      | —  | 1.25     | 1.25   |
|               | Pressure angle/(°)                      | 20°       | 20°  | 20°      | 20°    |
|               | Mass/kg                                 | 0.547     | 0.573  | 0.106    | 0.064  |
|               | Moment of inertia/kg • mm <sup>2</sup>  | 933.060   | 552.328  | 18.443   | 6.963  |
|               | Bearing stiffness/(N/μm)                | 170       | 109  | 126      | 108    |
|               | Torsional stiffness/(N/μm)              |           | $k_{su}^I = k_{cu}^I = 0$ $k_{ru}^I = 15750$   |          |        |
|               | Mesh stiffness/(N/μm)                   |           | $\bar{k}_m^I = 373.5$ $\bar{k}_{sn}^I = 322.8$ |          |        |
| Planet set II | Tooth width/mm                          | 17        | —  | 17       | 17     |
|               | Teeth                                   | 83        | —  | 33       | 25     |
|               | Pitch diameter/mm                       | 103.75    | —  | 41.25    | 31.25  |
|               | Base diameter/mm                        | 97.49     | 72.5   | 38.76    | 29.37  |
|               | Modulus/mm                              | 1.25      | —  | 1.25     | 1.25   |
|               | Pressure angle/(°)                      | 20°       | 20°  | 20°      | 20°    |
|               | Mass/kg                                 | 0.741     | 0.613  | 0.143    | 0.086  |
|               | Moment of inertia/ kg • mm <sup>2</sup> | 1277.185  | 730.328  | 27.812   | 11.145 |

|                            |      |  |   |     |
|----------------------------|------|--|---|-----|
| Bearing stiffness/(N/μm)   | 0.31 | 109  | 126   | 108 |
| Torsional stiffness/(N/μm) |      | $k_{su}^{\text{II}} = k_{ru}^{\text{II}} = 0$      | $k_{cu}^{\text{II}} = 6850$                       |     |
| Mesh stiffness/(N/μm)      |      | $\bar{k}_{rm}^{\text{II}} = 505.3$                 | $\bar{k}_{su}^{\text{II}} = 433.8$                |     |
| Tooth width/mm             | 23   | —  | 23  | 23  |
| Coupling stiffness/(N/μm)  |      | $k_{ssu}^{\text{I}} = k_{ssu}^{\text{II}} = 151.0$ | $k_{cru}^{\text{I}} = k_{cru}^{\text{II}} = 5630$ |     |
| Contact ratios             |      | $c_s^{\text{I}} = c_s^{\text{II}} = 1.66$          | $c_r^{\text{I}} = c_r^{\text{II}} = 1.79$         |     |

The vibration displacement time-domain curves of the ring gear of planet set I and II are shown in figure 2 and figure 3, where the negative value indicates the vibration displacement direction is opposite to the specified positive direction in the dynamic model. It can be known that the vibration displacements of each stage ring gear show fluctuation trends, in generally. The vibration displacement amplitudes of the ring gear of planet set I in the x, y translational directions are clearly more than in the u torsional direction, which in the y translational direction are more than in the x translational direction, it is illustrated that the dynamic load acting on the support bearing of planet with the ring gear of planet set I meshing in the y translational direction is more than in the x translational direction. The vibration displacement amplitudes of the ring gear of planet set II in the x, y translational directions are clearly less than in the u torsional direction, which illustrated that the vibration displacement of the ring gear of planet set II is significantly affected by torque.

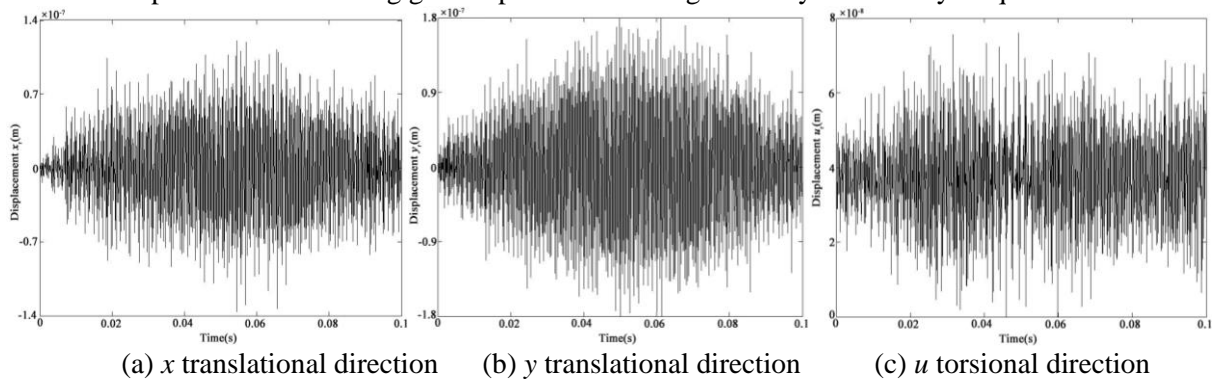


**Figure. 2** Vibration displacement time-domain curves of the ring gear of planet set I .

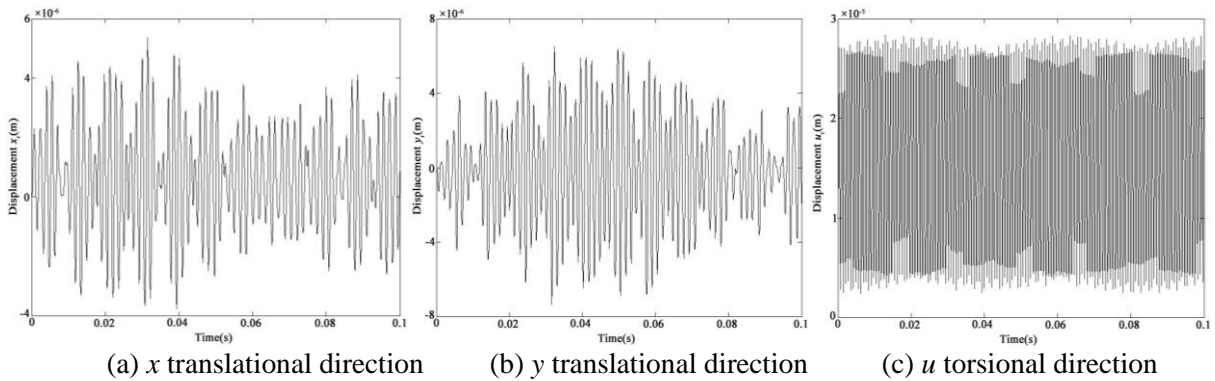


**Figure. 3** Vibration displacement time-domain curves of the ring gear of planet set II .

The vibration displacement frequency-domain curves of the ring gear of planet set I and II are shown in figure 4 and figure 5, in which  $f_m, f_h$  ( $h=r, c, s, p$ ) are meshing fundamental frequency and rotating frequency of each stage component  $h$ , respectively. As shown in figure 4(a), it can be known that the combination frequencies  $f_m/2 - f_s - 2f_c, 2f_m - f_p - 2f_s, 5f_m \pm 3f_p$  and  $3f_m, 5f_m$  appear in low-frequency, the vibration response peak at  $3f_m$ ; The odd multiple meshing fundamental frequencies are

main components in middle-frequency, such as  $7f_m$ ,  $9f_m$  and  $11f_m$ , where the vibration response peak at  $7f_m$ ; Except  $13f_m$  and the combination frequency  $13f_m + 3f_p - 3f_c$  appearing in high-frequency, the combination frequency  $12f_m + f_p + f_s$  is main component. As shown in figure 4(b), except  $5f_m$  and the combination frequency  $5f_m \pm 3f_p$ ,  $2f_m + 2f_p - 2f_s$ ,  $f_p - 2f_s$  appear in low-frequency, the meshing fundamental frequency  $f_m$  also appears, but the vibration response peak at  $3f_m$ ; Except the odd multiple meshing fundamental frequencies appearing in middle-frequency, the combination frequency  $8f_m - f_p + f_s$  also appears, the vibration response peak at  $7f_m$ ; The combination frequencies  $13f_m + f_p - f_s$  and  $14f_m - f_p - f_s$  appear in high-frequency; As shown in figure 4(c), the combination frequencies  $f_s - 3f_c$ ,  $5f_m + f_p + 2f_s$  and  $13f_m$  appear in low, middle and high-frequency of torsional direction, but the vibration displacement amplitudes are more.

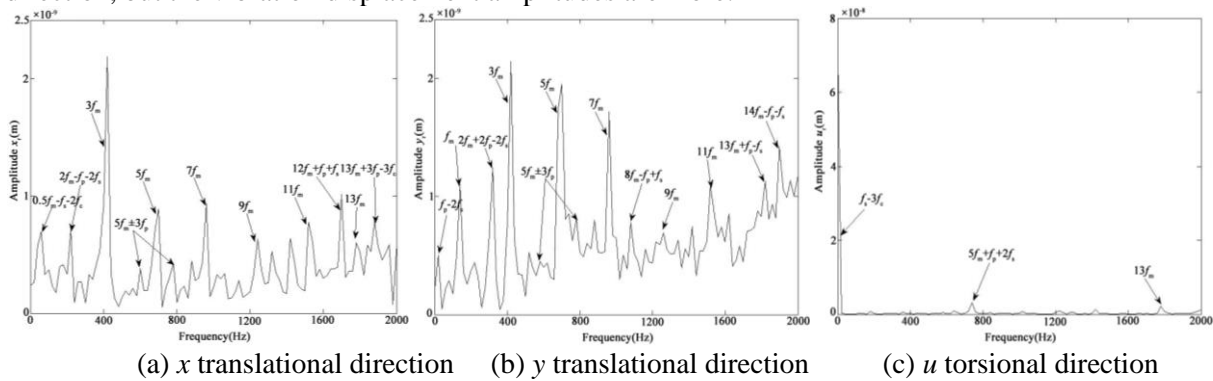


**Figure. 4** Vibration displacement frequency-domain curves of the ring gear of planet set I .

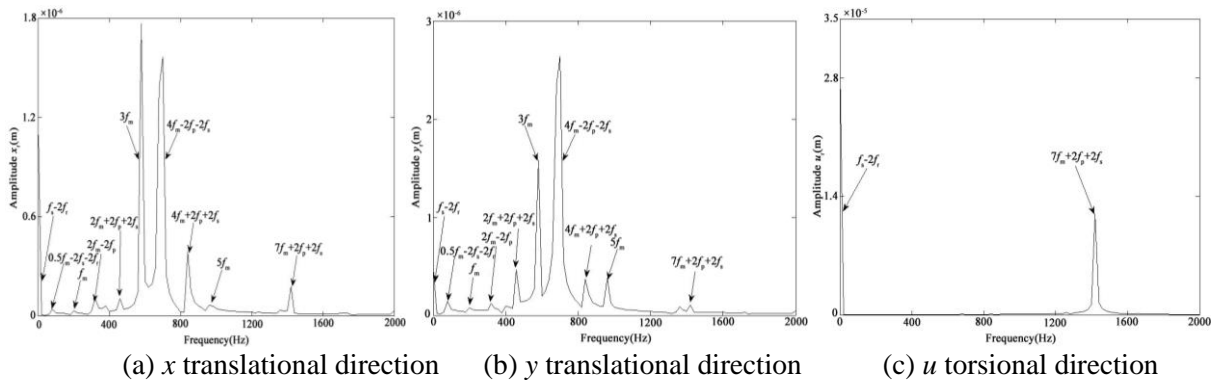


**Figure. 5** Vibration displacement frequency-domain curves of the ring gear of planet set II .

As shown in figure 5(a) and 5(b), it can be found that the spectra characteristic of the vibration displacements of the ring gear of planet set II are similar in the x and y translational direction. Except the combination frequencies  $f_s - 2f_r$ ,  $f_m/2 - 2f_s - 2f_r$ ,  $2f_m - 2f_p$  and  $2f_m + 2f_p + 2f_s$  appearing in low-frequency, the meshing fundamental frequency  $f_m$  also appear, the vibration response peak at  $3f_m$  in the x translational direction, but in the y translational direction the vibration response peak at  $4f_m - 2f_p - 2f_s$ ; Except the combination frequencies  $4f_m + 2f_p + 2f_s$  and  $7f_m + 2f_p + 2f_s$  appearing, meanwhile  $5f_m$  also appears in middle-frequency; The multiple meshing fundamental frequencies and rotating frequency of each stage component don't appear in high-frequency. As shown in figure 5(c), the combination frequencies  $f_s - 2f_c$  and  $7f_m + 2f_p + 2f_s$  appear in the low, middle-frequency, the meshing



fundamental frequency and rotating frequency of each stage component don't appear obviously in high-frequency.

#### 4. Conclusions

The dynamic responses of two-stage planetary transmission are solved by the Runge-Kutta method considering each stage internal and external time-varying mesh stiffness, which base on the lumped parameter-rigid elastic coupled dynamic model of two-stage planetary transmission for a hybrid car, the translational and torsional vibration displacements of each stage ring gear are obtained and the time-frequency responses are analyzed. The vibration displacements of each stage ring gear are affected differently in time-domain, the translational vibration displacement of the ring gear of planet set I are obviously more than the torsional vibration displacement, but it is opposite for the ring gear of planet set II; The translational and torsional vibration responses of each stage ring gear arrive the peak in low-frequency.

#### References

- [1] Y T Sun and H T Zhang 2011 *J. Heilongjiang Institute of Technol.* **25** 13–16 (in Chinese)
- [2] Y T Luo and Y S Chen 2012 *J. Mech. Engineering.* **48** 70–75 (in Chinese)
- [3] A Kahraman 1994 *J. Sound Vib.* **173** 125–130
- [4] Y M Song, W D Xu, C Zhang and S Y Wang 2006 *J. Mech. Engineering.* **42** 16–21 (in Chinese)
- [5] F H Duan, Q C Hu and C X Xie 2010 *J. Mech. Engineering.* **46** 62–67 (in Chinese)
- [6] J Lin and R G Parker 1999 *ASME J. Vib. Acoust.* **121** 316–321
- [7] T M Ericson and R G Parker 2013 *J. Vib. Acoust.* **135** 061002–1–13
- [8] D R Kiracofe and R G Parker 2007 *J. Vib. Acoust.* **129** 1–16
- [9] C G Cooley and R G Parker 2012 *J. Vib. Acous.* **134** 061014–1–11
- [10] J Lin and R G Parker 2002 *J. Sound and Vib.* **249** 129–145
- [11] C G Cooley and R G Parker 2013 *Int. J. Mech. Sci.* **69** 59–71
- [12] T Hidaka, Y Terauchi and K Nagamura 1979 *Bulletin of the JSME.* **22** 1142–49
- [13] J P Vaujany and H C Kim 1996 *ASME Design Engineering Division.* **88** 73–80
- [14] A Kahraman and S Vijayakar 2001 *J. of Mech. Design.* **123** 408–415
- [15] A Kahraman, A A Kharazi and M Umrani 2003 *J. Sound Vib.* **262** 752–768
- [16] X H Wu and R G Parker 2008 *J. Applied Mech.* **75** 0310141–12
- [17] R G Parker and X H Wu 2010 *J. Sound Vib.* **329** 2265–75
- [18] R G Parker and X H Wu 2012 *J. Vib. Acoust.* **134** 0410111–11
- [19] J Zhang, Y M Song and J J Wang 2009 *J. Mech. Engineering.* **45** 29–36 (in Chinese)
- [20] J Zhang, X Z Liu, Y Jiao and Y M Song 2014 *J. Mech. Engineering.* **50** 104–112 (in Chinese)
- [21] T Qing, W L Sun and J X Zhou 2015 *J. Xi'an Jiaotong University.* **49** 113–120 (in Chinese)
- [22] H Y Bao, X J Zhou, R P Zhu and F X Lu 2016 *J. Central South University (Sci. Technol.).* **47** 3005–10 (in Chinese)
- [23] J Y Li, Q C Hu, M Chai and X F Peng 2017 *J. Donghua University(Eng. Ed).* **34** 102–110
- [24] J Y Li and Q C Hu 2016 *Proc. Int. Conf. ASIAN MMS 2016& CCMMMS 2016 (Guangzhou)* vol 408 pp 1023–1042